

# Lab on a Chip

Accepted Manuscript



This is an *Accepted Manuscript*, which has been through the Royal Society of Chemistry peer review process and has been accepted for publication.

*Accepted Manuscripts* are published online shortly after acceptance, before technical editing, formatting and proof reading. Using this free service, authors can make their results available to the community, in citable form, before we publish the edited article. We will replace this *Accepted Manuscript* with the edited and formatted *Advance Article* as soon as it is available.

You can find more information about *Accepted Manuscripts* in the [Information for Authors](#).

Please note that technical editing may introduce minor changes to the text and/or graphics, which may alter content. The journal's standard [Terms & Conditions](#) and the [Ethical guidelines](#) still apply. In no event shall the Royal Society of Chemistry be held responsible for any errors or omissions in this *Accepted Manuscript* or any consequences arising from the use of any information it contains.

Cite this: DOI: 10.1039/c0xx00000x

www.rsc.org/xxxxxx

ARTICLE TYPE

## StyletChip: A microfluidic device for recording host invasion behaviour and feeding of plant parasitic nematodes

Chunxiao Hu<sup>a</sup>, James Kearns<sup>b</sup>, Peter Urwin<sup>c</sup>, Catherine Lilley<sup>c</sup>, Vincent O' Connor<sup>b</sup>, Lindy Holden-Dye<sup>\*b</sup>, and Hywel Morgan<sup>a</sup>

5 Received (in XXX, XXX) Xth XXXXXXXXXX 20XX, Accepted Xth XXXXXXXXXX 20XX

DOI: 10.1039/b000000x

Plant parasitic nematodes (PPNs) infest the roots of crops and cause global losses with a severe economic impact on food production. Current chemical control agents are being removed from use due to environmental and toxicity concerns and there is a need for new approaches to crop protection. A key feature of parasitic behaviour for the majority of PPNS is a hollow stomastyle or odontostyle required for interaction with the host plant and feeding. This lance-like microscopic structure, often called a stylet, protrudes from the mouth of the worm and thrusts in a rhythmic manner to stab the host root. Studying stylet activity presents technical challenges and as a consequence the underlying biology is poorly understood. We have addressed this by designing a microfluidic chip which traps the PPN *Globodera pallida* and permits the recording of an electrophysiological signal concomitant with stylet thrusting. The PDMS chip incorporates a precisely designed aperture to trap the nematode securely around a mid-point of its body. It is fabricated using a novel combination of conventional photolithography and two photon polymerization. The chip incorporates valves for rapid application of test compounds and integral electrodes to facilitate acquisition of electrical signals. We show that stylet thrusting can be induced by controlled application of 5-HT (serotonin) to the worm. Each thrust and retraction produces an electrical waveform that characterises the physiological activity associated with the worm's behaviour. The ability to reproducibly record the stylet activity of PPNS provides a new platform for nematicide screening that specifically focuses on a behaviour that is integral to the parasite host interaction. This is the first report of a microfluidic chip capable of electrophysiological recording from nematodes other than *Caenorhabditis elegans*. The unique approach is optimised for trapping and recording from smaller worms or worms with distinct anterior body shapes and may be applied to other species of economic or medical importance.

### Introduction

Plant parasitic nematodes (PPNs) are nematode worms that infest the roots of their host plants impairing plant viability, reducing the yield of crops and threatening food security. They have a significant severe global economic impact as most major food crops are susceptible to infestation by at least one nematode species. The most damaging and widespread of all PPNS are sedentary endoparasites<sup>1</sup> that include the root knot nematodes, *Meloidogyne spp.* and the cyst nematodes such as *Globodera spp.* Root knot nematodes and cyst nematodes hatch at the 2nd juvenile stage outside of a host plant. On locating a suitable host the juveniles invade the root and find an appropriate location to establish a feeding site, where they will develop through to adulthood and reproduce. Despite their economic importance, much remains unknown about these sedentary endoparasitic nematodes, including the neural mechanisms underlying the behaviours that allow host plant location and invasion that are essential to the parasitic life cycle. A greater understanding of PPN neurobiology would facilitate the development of new

agents for crop protection: Such approaches are currently very limited due to the strict regulation of environmentally-damaging nematicides<sup>2,3</sup>.

All sedentary endoparasitic nematodes possess a stylet, a hollow protrusible spear that is integral to hatching of the juvenile larva, J2, from the egg, invasion of the host plant and in feeding of the parasitic stages once the nematode is established within the host. Host plant invasion by cyst nematodes is accomplished by movements of the stylet back and forth to allow mechanical piercing of the root epidermis and permit entry<sup>4,5</sup>. During invasion the stylet also delivers enzymes originating from the oesophageal glands to aid plant cell wall degradation<sup>6</sup>. Once the nematode has migrated to the vascular cylinder of the root, which contains xylem and phloem tissue, a parenchymous cell is selected, into which the stylet is inserted for several hours; secretions from the stylet are required to establish the parasitic feeding site<sup>7</sup>.

It is clear that the behaviour of the stylet is essential for plant parasitism and yet relatively little is known about the molecular and physiological mechanisms that underpin its activity. Its

activity is dependent on rhythmic muscular contraction supported by neural signalling. Further, sensory modulation is implied through the dependence of this behaviour on the host plant however the neurochemical basis of this is poorly understood. One observation is that exogenous compounds including 5-hydroxytryptamine (5-HT or serotonin) stimulate stylet thrusting suggesting a monoamine modulation of the core physiology<sup>8, 9</sup>. Thus, although currently limited in scope, published data on the physiological analysis of stylet behaviour highlights pharmacological intervention of its activity as a potentially effective means of crop protection by reducing hatching, host plant invasion and feeding. An important bottle neck is developing approaches to delineate the physiological basis of the stylet function.

Whilst the frequency of stylet thrusts can be scored visually this approach lacks precision and detail. An improvement on this involves glass suction microelectrodes placed over the mouth of the worm to obtain extracellular electrophysiological recordings: This has been achieved for J2 larvae of the PPN *Globodera rostochiensis*<sup>10</sup>. Signals corresponding to stylet protrusion and retraction stimulated by the neurotransmitter 5-HT were observed<sup>10</sup>. However, there have been very few functional or pharmacological studies on stylet activity<sup>9, 11</sup>.

In this study we have designed a microfluidic chip that permits electrophysiological recordings of stylet activity but which circumvents the need for a conventional glass microelectrode and the challenges of micro-manipulation. It traps the worm whilst simultaneously acting as the platform for recording the electrical signals and can be paired with visual inspection or video recording of the accompanying stylet thrusts. The device, StyletChip, provides robust and reproducible signals that are comparable to those obtained from conventional glass microelectrode electrophysiological recordings. The new chamber has been dovetailed with a microfluidic platform previously designed for recording from adult *Caenorhabditis elegans*<sup>12</sup> that adds features for rapid perfusion of chemicals to the stylet. This combination provides the potential for chemical screens. In addition, we show that the electrophysiological recordings from StyletChip harbour detail that cannot be obtained by visual inspection of stylet thrusting behaviour. We discuss the potential this may have for providing an experimental platform to provide fundamental insight into the neurobiology of the oesophageal/stylet system of the PPNs.

## Material and Methods

### Design of the StyletChip

A number of different microfluidic chambers have been described for trapping and investigating the biology of the nematode *C. elegans*<sup>13-24</sup>, and more recently two devices have been designed for electrophysiological recording of pharyngeal activity<sup>12, 25</sup>. However, compared to young adult *C. elegans*, the J2 stage of *G. pallida* is about a quarter of the overall size (~430  $\mu\text{m}$  long and ~23  $\mu\text{m}$  in diameter; Fig. 1). This presents a much greater challenge in terms of manipulation and precise trapping. We have previously shown that in order to record electrophysiological signals corresponding to the pharyngeal activity of *C. elegans* it is necessary to trap the worm in an aperture that fits snugly

around the nose of the worm<sup>12</sup>. This provides an electrical seal separating the anterior and posterior sections of the worm and, analogous to the classic sucrose gap technique<sup>26</sup>, enables recording of the electrical signals arising from excitable tissues within the worm as a potential difference between the anterior and posterior chambers of the microfluidic device. The *C. elegans* trap, NeuroChip, was fabricated using conventional photolithography<sup>12</sup> but this technique cannot create an optimised aperture shape for smaller nematodes. To address this issue, we have used a pseudo-three dimensional high resolution lithographic approach, provided by the technique of two-photon polymerization<sup>27-29</sup>. Two-photon polymerization provides a means of activating chemical or physical processes with high spatial resolution in three dimensions, because the two-photon absorption probability depends quadratically on intensity<sup>30</sup>. It can generate any kind of 3D structure based on computer generated 3D models with a resolution of around 100 nm and the fabrication process is simple and fast<sup>31</sup>. This new approach is used to make small shaped features in a negative photoresist and thereby microfluidic devices with different shapes.

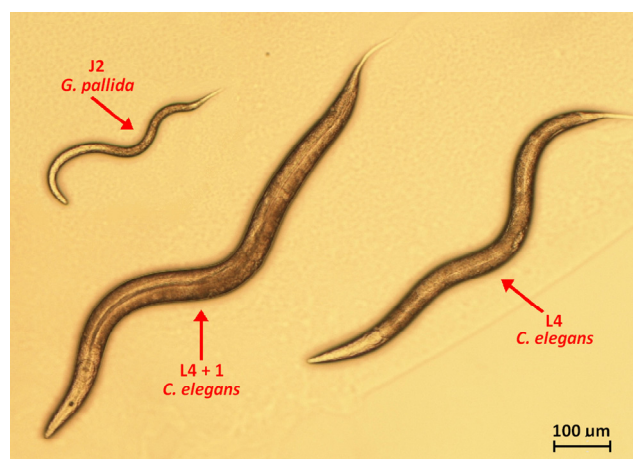


**Fig. 1** Micrographic image shows the difference of the dimensions of the young adult *C. elegans*, L4 *C. elegans* and J2 *G. pallida*.

### Fabrication of the device

The StyletChips were fabricated from PDMS using soft lithography with a mold made using a two-step process. High resolution features capable of trapping the worm were made using two-photon lithography, whilst the remainder of the microfluidic network, including the microfluidic valves were made using conventional photolithography. Unlike conventional

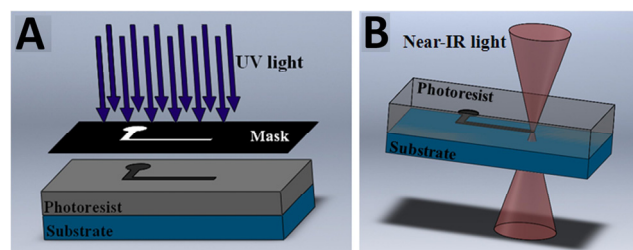


**Fig. 2** Two different approaches to the polymerization of a negative photoresist. (A) Conventional UV lithography, where light is projected through a shadow mask onto a photosensitive material. (B) Two-photon polymerization: High resolution 3-D structures are written in the volume of the photoresist using a pulsed near-IR laser.

lithography which uses UV light to expose a negative resist through a shadow mask (Fig. 2A), two-photon polymerization uses a pulsed ultra-short near-infrared (IR) laser with a wavelength of around 780 nm. This light is focused inside the photoresist and initiates highly localised polymerisation<sup>27</sup> (Fig. 2B), enabling the writing of sub-micron features. Fabrication of a computer-generated 3-D structure is achieved by raster scanning the laser in the volume of the photosensitive material<sup>29</sup>. With two-photon polymerization, miniaturised structures ranging from hundreds of nanometres to several micrometres of different irregular shapes can be made, with a fast design to production cycle.

The SU8 mold was made as follows. First the high resolution trapping channel was made using a two-photon tool (Nanoscribe, GmbH, Germany). The Nanoscribe was used to create a semi-cylindrical shaped trapping channel (see Fig. 3A). A 3-D model of the trap was designed in CAD (Solidworks) and exported to the Nanoscribe. A thin layer of SU8-25 was spun onto a glass wafer to a thickness of 25  $\mu\text{m}$  and soft baked, and then processed with the Nanoscribe. An example of a trap made in SU8 is shown in Fig 3B. The trap was designed to accommodate *J2 G. pallida*, and several different trap sizes were made and tested to obtain the optimum dimensions. Two trap heights were tested, 9.5  $\mu\text{m}$  and 11  $\mu\text{m}$  and the following left width-right width, length combinations ( $\mu\text{m}$ ) with respect to Fig. 3A: 13-16  $\times$  15; 13-20  $\times$  15; 13-13  $\times$  20; 15-15  $\times$  20; 13-10  $\times$  20; 15-10  $\times$  20; 17-10  $\times$  20; 20-9  $\times$  20. The optimal design was 20  $\mu\text{m}$  long, 11  $\mu\text{m}$  high and tapered from 10  $\mu\text{m}$  to 15  $\mu\text{m}$  along its width from left to right (measured by SEM from the SU8 master; see Fig. 3).

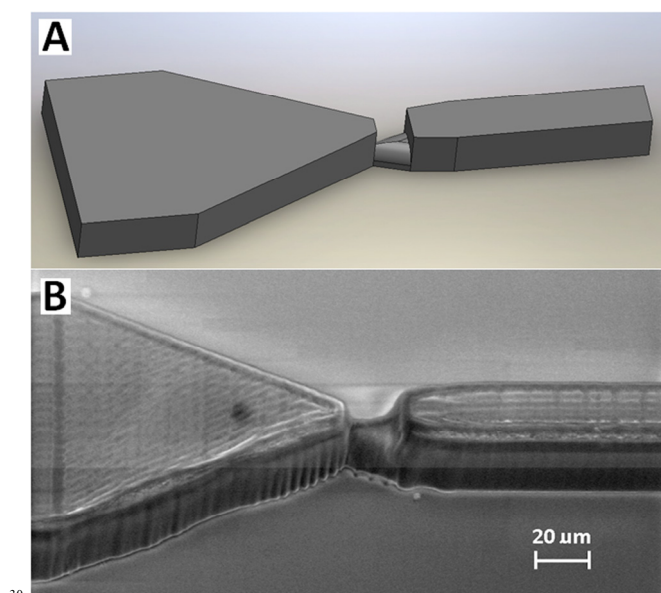


**Fig. 3** (A). CAD image of the 3-D structure that traps *J2 G. pallida*. (B) SEM image of the semi-cylindrical trapping channel. The rounded shape (written with the Nanoscribe) provides a tight fit to the contours of the worm.

The microfluidic channels that were used to deliver worms and drugs to the device were made in the same SU8 using conventional photolithography. A standard mask was used to define the microfluidic channels except the trapping region (see ESI 1 for design). After writing the trap region with Nanoscribe,

the exposed SU8 was left undeveloped. In order to make the trapping channel visible for ease of alignment the contrast between the exposed and unexposed SU8 was increased by baking the substrate at 65°C for 30 seconds. After aligning the mask with the trap and exposing the remainder of the SU8, the entire wafer was developed and hard baked. An example of an SU8 master made this way is shown in ESI 2. As the photograph shows, a small amount of SU8 overlaps the high resolution 3-D trap, but this makes no difference to the performance of the final device (Fig. 4A).

The flow of liquid in this microfluidic network is controlled by a set of valves, as shown schematically in Fig. 4B. The final design of valves follows our previously published system for *C. elegans*<sup>12</sup>. The valve layer was made using SU8-50 spun to a thickness of 60  $\mu\text{m}$ . The final chip also includes integrated platinum microelectrodes for electrical recording. The design has an additional feature optimised for studies on PPNs which allows drugs and chemicals to be applied to either side of the trap. This means that chemicals and drugs can be applied to the mouth of the trapped worm regardless of which orientation the worm enters the device (head first apply chemicals via drug port 2; tail first apply chemicals via drug port 1, Fig. 4B).

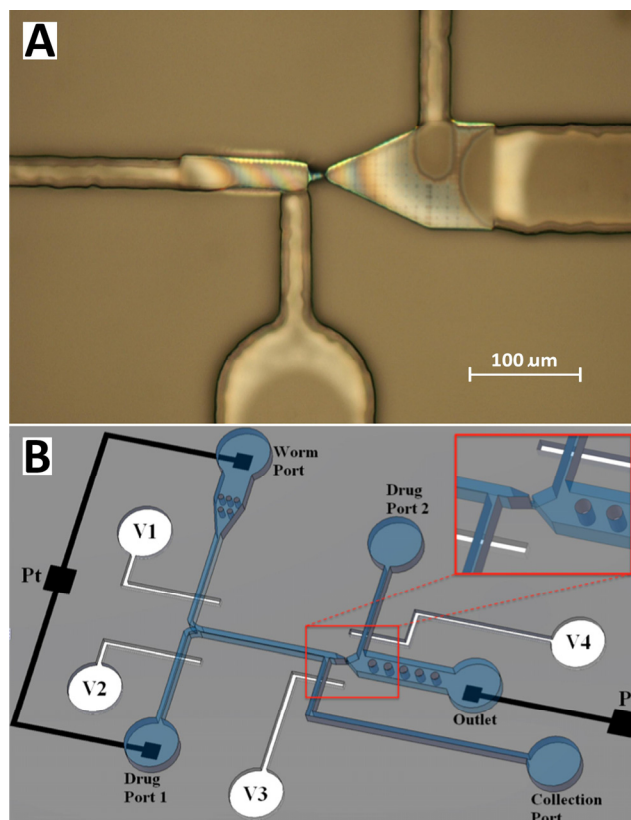


**Fig. 4** (A) Photograph of the SU-8 master that is used to fabricate the StyletChip. (B) Schematic layout of the chip showing the integrated Pt electrodes (at inlet and outlet), the trap region (inset) and the four valves (V1, V2, V3 and V4) used to control worm loading (V1), chemical or drug delivery (V2 and V4) and worm retrieval (V3).

To make the StyletChip, PDMS is poured over the SU8 microfluidic master and cured. The valve layer is made separately by spin coating liquid PDMS over the second SU8-50

master, leaving a 75  $\mu\text{m}$  thin membrane on top of the features. The entire device is assembled by removing the cured microfluidic layer from the SU8 mold and bonding this to the valve layer. The entire structure is then removed from the second mold and bonded to a glass wafer which includes the Pt electrodes. Prior to bonding all holes for tubing and electrodes were cut in the PDMS.

To record the electrical activity from the worm, the electrodes were connected to an AxoClamp 2A amplifier. Where indicated in the results, low frequency drift was removed by Clampfit 9.0 (Axon Instruments) with a Highpass Bessel filter and 0.5 Hz 230 dB cut-off frequency. The integrated electrodes simplify the experimental set-up compared to classical external microelectrodes without affecting signal acquisition<sup>12</sup>. Signals were analysed manually in combination with AutoEPG software<sup>32</sup>. To ensure accurate detection of all the waveforms in a recording each waveform was annotated manually within the AutoEPG software programme and then the software was used to extract the average waveform rate and duration from the data set. Signal amplitudes were measured manually from the recordings.

J2 *G. pallida* were freshly hatched in potato root diffusate (1 part PRD to 3 parts distilled water) from sterilised, rehydrated cysts and maintained at room temperature in PRD as previously described<sup>33</sup>. Prior to the experiment the nematodes were washed in distilled water.

## Results and Discussion

### Electrophysiological recordings from *G. pallida*

Recordings were made from J2 *G. pallida* within 48 hours of hatching. Individual worms were suspended in Dent's saline (composition in mM; D-glucose 10, HEPES 10, NaCl 140, KCl 6, CaCl<sub>2</sub> 3, MgCl<sub>2</sub> 1, pH 7.4 with NaOH) and loaded into a StyletChip. The worm was pushed into the trapping region (see Fig. 4A) at a small constant positive pressure of (0.5mBar) through the use of four valves (V1, V2, V3, and V4 in Fig. 4B) which were actuated separately to control the bypass channels at a pressure of 2 Bar. During recording, either the drug port or the worm port remained open. Electrophysiological signals were then captured and either observed in real time or recorded for post hoc analysis. Drugs were applied from either drug port 1 or 2, depending on the orientation of the worm. After the recording, the worm could be either unloaded or collected from the collection port of the device. In the absence of any chemical stimulation, the stylet of J2 *G. pallida* is inactive: No stylet thrusts were observed visually and the electrophysiological recordings detected no waveforms.

Relatively consistent rhythmic thrusting could be induced by application of 5-HT and when 2 mM 5-HT was applied through the drug port this was accompanied by rhythmic electrical signals with a frequency of about 1Hz. No stylet thrusting was observed unless 5-HT was applied. The largest amplitude signals were recorded when the worm was held in the trapping channel about one third to one half of the distance along its body length, irrespective of the orientation of the worm (Fig. 5). In this configuration, the worm is trapped in the region of the

oesophageal bulb. Further studies are required to establish the contribution of the activity of this muscular organ to the waveform. Fig. 5A shows the signal from a worm trapped by its most anterior tip and Fig. 5B and C show the signal obtained from a worm trapped around the body that entered the device tail first and head first respectively. Following trapping worms could be released from the chip and were observed to move indicating they can survive the procedure.

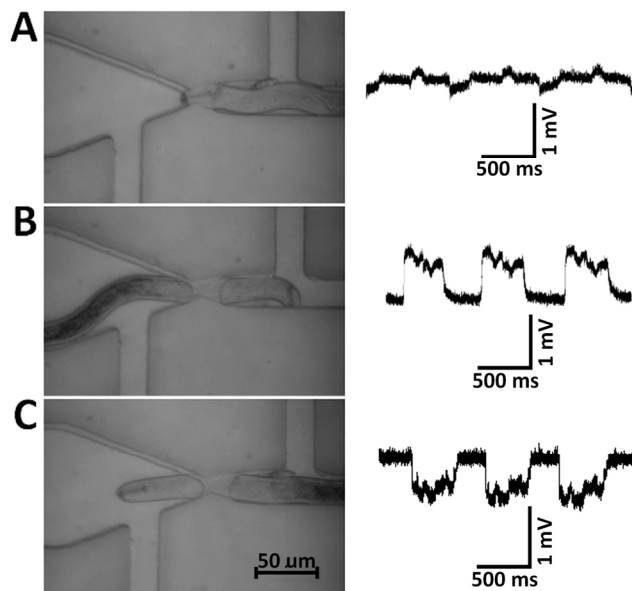


**Fig. 5** Different trapping positions of J2 *G. pallida* generate electrical signals with different amplitude in the presence of 2 mM 5-HT. (A) A nematode that was captured on the head in the trapping channel and the corresponding electrical activity. Nematodes that were captured on the body either tail first (B) or head first (C) in the trapping channel, and the corresponding electrical activity. The amplitude of signal obtained from the body is several times bigger than that from the trapped head.

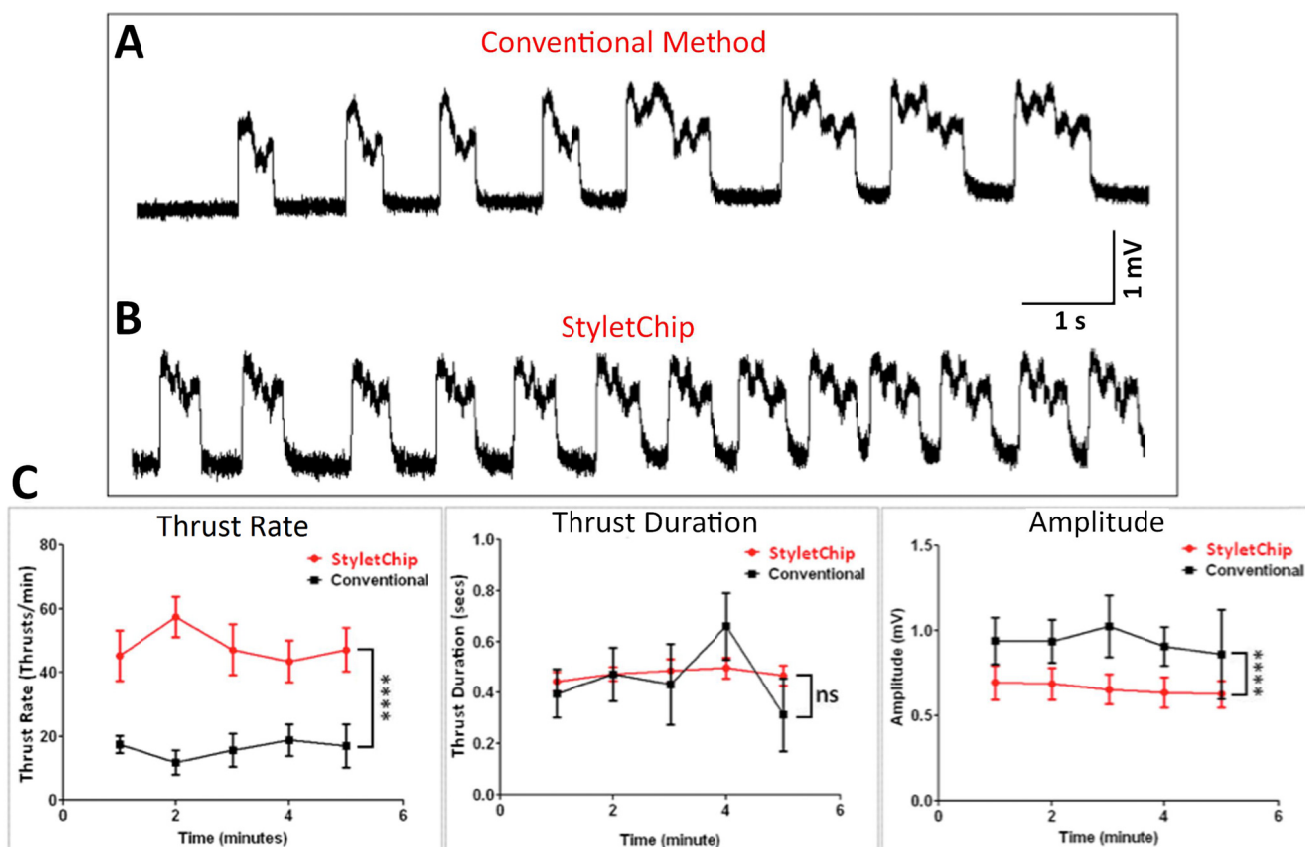


**Fig. 6** Comparison of the electrical signals obtained from J2 *G. pallida* in a Petri dish with extracellular glass microelectrodes (conventional method) and from StyletChip in 2 mM 5-HT. (A) Conventional electrical recordings. For these experiments individual J2 larvae were trapped on the end of a glass suction microelectrode filled with Dent's saline and connected to an Axoclamp 2B recording amplifier as previously described for *C. elegans*<sup>34</sup>. (B) An electrophysiological recording obtained from trapped J2 *G. pallida* with StyletChip. (C) Time courses of the frequency, duration, and amplitude, of the signals comparing the stability of recording with conventional microelectrode (n=5) and the StyletChip (n=9). Data are the mean  $\pm$  SEM.

### Comparison of StyletChip with conventional recordings

A previous study of the electrophysiological recording from J2 *G. pallida* used extracellular glass capillary suction electrodes placed on the anterior most tip of the worm<sup>10</sup>. Here we used a similar approach to make a direct comparison between signals acquired using StyletChip and glass microelectrodes. For both types of recordings very similar electrical signals were observed (Fig. 6; Table 1). However, the activity recorded in response to 2 mM 5-HT using StyletChip was consistently of a higher frequency and lower amplitude than that recorded from the conventional microelectrode involving bath application of the same dose of 5-HT. The lower amplitude of the signal in the StyletChip may indicate that the dimensions of the trapping aperture are still not optimal and further refinement of this may improve the amplitude of the waveform. The observation that the frequency of activity was higher in worms that were restrained in the microfluidic chamber compared to recordings made using suction electrodes is similar to the situation for electrophysiological recordings of *C. elegans* pharyngeal activity in a microfluidic device<sup>12</sup> and may reflect an effect of constrained movement on pharyngeal activity<sup>35</sup>.

**Table 1:** Characteristics of stylet associated activity recorded with StyletChip or conventional microelectrodes. Data are the mean  $\pm$  s.e.mean of recordings from 'n' J2 *G. pallida* worms. Each parameter was derived from AutoEPG analysis<sup>32</sup> of all the waveforms captured in a recording of 5 minutes or, for manual analysis, from 50 waveforms. Comparisons made by unpaired Student's t-test to the respective parameters for 1,2,3 conventional recording with 2 mM 5-HT, P<0.0001, P=0.7656 and P<0.0001 respectively. 'ns' not significant.

	StyletChip (n=9)	Conventional microelectrode (n=5)
<b>J2 <i>G. pallida</i></b>		
Thrust frequency (min <sup>-1</sup> )	48.04 $\pm$ 2.42 **** <sup>1</sup>	16.13 $\pm$ 1.19
Thrust duration (ms)	487.9 $\pm$ 6.1 ns <sup>2</sup>	455.0 $\pm$ 57.6
Amplitude (mV)	0.66 $\pm$ 0.013 **** <sup>3</sup>	0.93 $\pm$ 0.027

### Electrophysiological recordings inform on stylet behaviour

Three different kinds of electrical waveforms were observed from the trapped nematodes in StyletChip (Fig. 7): i) short thrust (ST) consists of a roughly square waveform of ~300 ms duration with a single, small, transient negative going potential (TP) interleaved between the upward deflection and return to baseline

ii) normal thrust (NT) is similar except it has a longer duration of ~ 500 ms and 2 to 3 transient negative going potentials (TPs) interleaved between the upward deflection and return to baseline  
 iii) long thrust (LT) which has the longest duration of over 1s and a number of transient negative going potentials (TPs) interleaved between the upward deflection and return to baseline. This classification is based on recordings from 9 worms with >50 waveforms per recording. Each worm can exhibit each of these waveforms however normal thrust is the most common type of waveform. In further studies it would be interesting to test whether or not the pattern of these waveforms was subject to pharmacological modulation to provide insight into the neurotransmitter signalling pathways that might underpin these events.

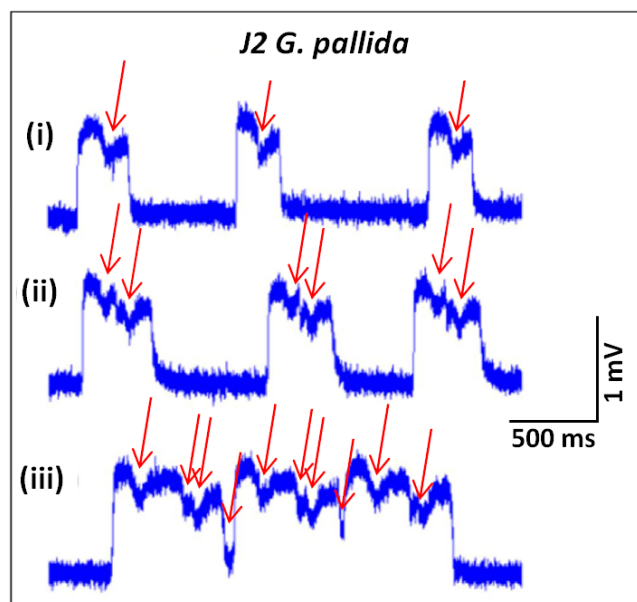


**Fig. 7** Three different waveforms observed during recordings with StyletChip on J2 *G. pallida*. (i) Short thrust (ST): only two peaks generated during one single thrust with duration of ~ 300 ms. (ii) Normal thrust (NT): two to three peaks generated during one single thrust with duration of ~500 ms. (iii) Rapid thrust (RT): several waveforms merged together to form one long thrust. Red arrows indicate the places of transient negative going potentials (TPs).

Whilst the signals recorded with the conventional microelectrode and StyletChip are similar in this study, they differ from an earlier report of conventional extracellular recordings from the anterior of the PPN *G. rostochiensis*<sup>36</sup>. These earlier recordings were of lower amplitude, 0.3 mV, and had a different waveform consisting of a fast positive going transient followed by a fast negative going transient. This difference might reflect species differences in stylet activity but a more likely explanation is that filtering of the *G. rostochiensis* signal produced the reported bi-directional waveform. Nonetheless, the duration of the waveform reporting on stylet thrusts for *G. rostochiensis* was similar to that for *G. pallida*.

In order to provide insight into the functional correlates of the electrophysiological recordings we performed simultaneous video capture. The stylet itself is very small and cannot be readily visualised in the StyletChip chamber. However, small swellings

at the caudal end of the stylet, called the stylet knob (dashed red line in Fig. 8) provide a reference point for the position of the stylet. During a stylet thrust the stylet knobs move anteriorly towards the mouth and during stylet retraction return to their resting position. The position of the stylet knobs of J2 *G. pallida* was viewed at  $\times 40$  magnification on a Zeiss Axiovert 200 inverted microscope (Carl Zeiss, Cambridge, UK) and recorded by a camera (ImagingSource DMK 31BU03 ALRAD Instrument, Newbury, UK). The correlation between stylet motion and electrical activity was recorded by screen capturing software (Screen Video Specialist, PingLu Software Studio, ZheJiang, China). Examination of the video on a frame to frame basis demonstrates a correlation between stylet knob movement and electrical signal (Fig. 8). The thrusting of the stylet triggers a positive deflection. The stylet remained extended throughout the duration of the waveform and returned to its resting position when the electrical signal returned to baseline.

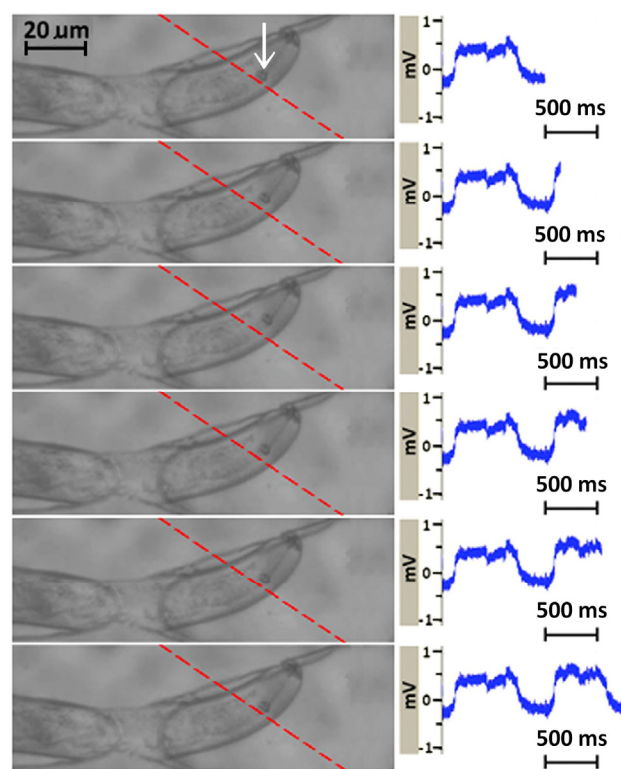


**Fig. 8** Video frames (80ms per frame) reveal the correlation between the stylet motion of J2 *G. pallida* and the electrophysiological waveform. The thrusting of stylet triggers a positive spike and the back motion leads the spike back to the baseline. Dashed red line indicates the original position of the stylet knobs. The white arrow indicates the one visible stylet knob.

This indicates that the electrophysiological recording provides a read-out of the frequency of stylet thrusts. Over and above this, there is further detail to the electrophysiological recordings that remains to be defined. These are the transient potentials (TPs) embedded within each waveform. Further studies are required to assign a functional identity to the TPs however a possibility is that they report activity of the median bulb, a muscular structure just posterior to the stylet which pumps food through to the oesophagus. The ability to use electrophysiological recordings from a PPN to precisely resolve the nature of stylet responses provides a new opportunity to study the physiology of the stylet,

and also possibly the median bulb: Physiology that is integral to the PPN parasitic lifestyle. PPNs can show oesophageal activity in the absence of stylet thrusting. Whilst we have not observed any electrophysiological evidence for this, the microfluidic chip provides a new opportunity to probe this biology.

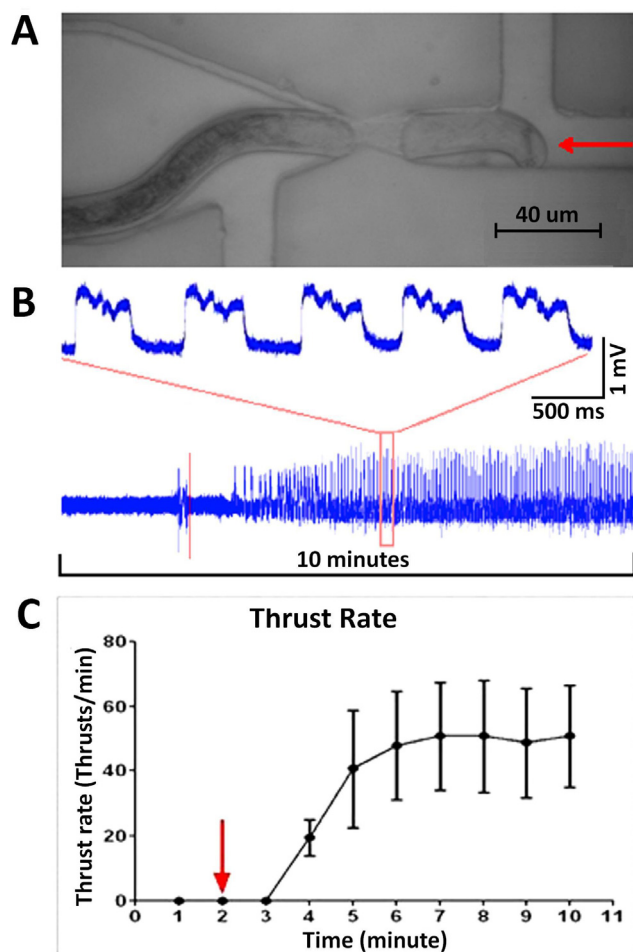


**Fig. 9** The response of J2 *G. pallida* to drug application in StyletChip. (A) Image of a trapped J2 *G. pallida* in the device. The nematode is trapped on the middle of the body. Red arrow indicates the direction of drug application (B) A sample of a recording obtained from drug diffusion assays. 2 mM 5-HT was applied at 2 minutes, indicated by the vertical red line. Low frequency drift was removed by Clampfit 9.0 (Axon Instruments) with a Highpass Bessel filter and 0.5 Hz -30dB cut-off frequency. (C) Response time to 5-HT in drug diffusion assays. Red arrow indicates the time point of 5-HT addition. Data are the mean  $\pm$  s.e.mean of recordings from 5 worms.

### The time-course of drug responses in StyletChip

The response of J2 *G. pallida* in StyletChip to timed application of 5-HT was tested. J2 *G. pallida* were loaded into the microfluidic chamber under constant positive pressure ( $\sim 0.2$  mBar) and electrophysiological recordings of baseline activity were obtained. For these studies the worms were loaded into the device tail first (Fig. 9A). In the absence of any chemical stimulation, no stylet thrusts and no electrical activity was recorded. After 2 minutes, 2 mM 5-HT was applied (from the drug port). Stylet activity was observed after a further 2 minutes (Fig. 9B).

The frequency reached its maximum three minutes after addition of the 5-HT (Fig. 9C), and the rate is similar to that obtained from worms which had been treated with 2 mM 5-HT prior to loading into the device (Table 1). The recording continued for a further 10 minutes, and the worm was then ejected from the device and another nematode loaded from the reservoir and the process repeated. During the recording the worm's head could move within the channel however this movement did not prevent the recording of a stable signal (Fig. 9B).

These experiments demonstrate the capability of StyletChip to measure responses to drugs with multiple worms. The 5-HT had to be applied to the anterior, mouth end of the worm in order to elicit a stimulatory response. In experiments in which the 5-HT was applied to the posterior end no stylet response or electrical signal was recorded even after 30 minutes application of 5-HT (data not shown). This suggests that 5-HT must either act on external chemoreceptors on the anterior of the worm or, more likely it gains access to the stylet and oesophageal system through the mouth of the worm.

### Conclusions

Earlier applications of microfluidic technology for electrophysiological recordings from nematodes have provided a platform for recording from the free-living nematode *C. elegans*<sup>12, 25</sup>. *C. elegans* does not possess a stylet and these previous electrophysiological recordings provided a read-out of the rhythmic contraction-relaxation cycle of the pharyngeal organ that underpins feeding behaviour. The success of the microfluidic approach for recording from the pharyngeal system of *C. elegans* prompted the investigation of designs for other species of nematode, in particular those that are pests and parasites. The PPNs that infest crops present particular challenges as the infective stages are considerably smaller than *C. elegans*. Our approach to this has been to use two photon polymerisation in order to generate a sufficiently small rounded trapping aperture to match the contours of the worm. We have combined this with conventional photolithography to incorporate flow channels and a valve system. The resulting device, StyletChip, records an electrophysiological signal that reports on the frequency and duration of the nematode's stylet thrusts. The fact that the frequency of the electrophysiological signal correlates with the visual observation of the frequency of stylet thrusts and furthermore that 5-HT stimulates the frequency stylet thrusting whilst at the same time inhibiting worm movement<sup>8</sup> indicates that the electrophysiological signal recorded in StyletChip reports stylet activity and not body wall muscle movement. As noted in the introduction, stylet thrusting is essential to enable the worm to pierce the root epidermis and enter the host plant<sup>4, 5</sup>. Moreover, the electrophysiological signals have resolvable sub-features which we argue have the potential to provide a route to inform on important functional aspects of the nematode's pharyngeal/oesophageal physiology in the same way that EPG recordings have provided this information for *C. elegans*<sup>37</sup>. For PPNs, this aspect of their biology is very poorly understood and yet it is integral to the nematode's parasitic lifestyle for example in regulating the secretion ('spitting') of enzymes originating

from the oesophageal glands which aid plant cell wall degradation<sup>6</sup>.

The ability to make recordings from PPNs using a microfluidic platform circumvents the technical challenges presented by conventional electrophysiological approaches and opens the way for wider adoption of this experimental technique. In particular StyletChip would be suitable for studies aimed at defining the actions of chemicals on stylet and/or median bulb activity with a view to developing new chemicals for crop protection.

Recordings using StyletChip may be made regardless of whether the worm enters the channel head or tail first. Unlike the microfluidic device designed for recording *C. elegans* EPG waveforms<sup>12</sup> it is not necessary to control the orientation of the worm as it enters the device: Provision of two routes for chemical application to the channel means that chemicals can be applied to the head regardless of the orientation of the worm.

The modular design of StyletChip means that by simply changing the dimensions of the independently engineered trapping aperture it may be adapted to trap and record electrophysiological signals from other species of parasitic nematode that are otherwise too small to study easily with conventional approaches. The PPNs vary in length from 250  $\mu\text{m}$  up to 12 mm but their diameter is more consistent. It is the diameter that dictates the size of the chip aperture so one can envisage that the same device might accommodate various species of PPN.

Overall the paper reports on an important technical advance to the investigation of feeding structures in plant parasitic nematodes, and potentially other microscopic parasites with electrically recordable bio-signals that are otherwise intractable to precise and quantifiable measurement.

## Acknowledgements

This project was financed in part through Biotechnology and Biological Sciences Research Council UK (BBSRC) Grant no BB/J006890/1.

## Notes and references

<sup>a</sup> Faculty of Physical Sciences and Engineering, and Institute for Life Sciences, University of Southampton, Southampton, SO17 1BJ, United Kingdom. Fax: 44 (0)2380 593029; Tel: 44 (0)2380 593330; E-mail: hm@ecs.soton.ac.uk

<sup>b</sup> Centre for Biological Sciences, Institute for Life Sciences, University of Southampton, Southampton, SO17 1BJ, United Kingdom. Fax: 44 (0)2380 595159; Tel: 44 (0)2380 599006; E-mail: lmhd@soton.ac.uk

<sup>c</sup> Centre for Plant Sciences, School of Biology, University of Leeds, Leeds, LS2 9JT, UK. Tel: +44 (0)113 3432909; E-mail: P.E.Urwin@leeds.ac.uk

\*Corresponding author

† Electronic Supplementary Information (ESI) available: [ESI 1: The design of the mask which was used to define the microfluidic channels except the trapping. ESI 2: This shows an example of an SU8 master which was made by aligning the mask with the trapping channel and exposing the remainder of the SU8. Subsequently the entire wafer was developed and hard baked. See DOI: 10.1039/b000000x/]

1. K. R. Barker and S. R. Koenning, *Annu Rev Phytopathol*, 1998, 36, 165-205.

2. K. Steenland, *BMJ*, 1996, 312, 1312-1313.

3. J. F. Risher, F. L. Mink and J. F. Stara, *Environ Health Perspect*, 1987, 72, 267-281.

4. V. M. Williamson and C. A. Gleason, *Curr Opin Plant Biol*, 2003, 6, 327-333.

5. U. Wyss and U. Zunke, *Revue Nematol*, 1986, 9, 153-165.

6. G. Smant, J. P. W. G. Stokkermans, Y. T. Yan, J. M. de Boer, T. J. Baum, X. H. Wang, R. S. Hussey, F. J. Gommers, B. Henrissat, E. L. Davis, J. Helder, A. Schots and J. Bakker, *P Natl Acad Sci USA*, 1998, 95, 4906-4911.

7. U. Wyss, *Fund appl nematol*, 1992, 15, 75-89.

8. E. P. Masler, *J Helminthol*, 2007, 81, 421-427.

9. L. Holden-Dye and R. J. Walker, *Invert Neurosci*, 2011, 11, 9-19.

10. R. N. Rolfe and R. N. Perry, *Nematology*, 2001, 3, 31-34.

11. R. N. Perry, *Int J Parasitol*, 2001, 31, 909-918.

12. C. Hu, J. Dillon, J. Kearns, C. Murray, V. O'Connor, L. Holden-Dye and H. Morgan, *Plos One*, 2013, 8, e64297.

13. J. N. Stirman, M. Brauner, A. Gottschalk and H. Lu, *J Neurosci Meth*, 2010, 191, 90-93.

14. T. V. Chokshi, A. Ben-Yakar and N. Chronis, *Lab Chip*, 2009, 9, 151-157.

15. S. E. Hulme, S. S. Shevkopylas, J. Apfeld, W. Fontana and G. M. Whitesides, *Lab Chip*, 2007, 7, 1515-1523.

16. S. E. Hulme, S. S. Shevkopylas, A. P. McGuigan, J. Apfeld, W. Fontana and G. M. Whitesides, *Lab Chip*, 2010, 10, 589-597.

17. R. Sznitman, M. Gupta, G. D. Hager, P. E. Arratia and J. Sznitman, *Plos One*, 2010, 5, e11631.

18. J. Krajniak, Y. Hao, H. Y. Mak and H. Lu, *Lab Chip*, 2013, 13, 2963-2971.

19. T. V. Chokshi, D. Bazopoulou and N. Chronis, *Lab Chip*, 2010, 10, 2758-2763.

20. C. B. Rohde, F. Zeng, R. Gonzalez-Rubio, M. Angel and M. F. Yanik, *Proc Natl Acad Sci U S A*, 2007, 104, 13891-13895.

21. K. Chung, M. M. Crane and H. Lu, *Nat Methods*, 2008, 5, 637-643.

22. S. X. Guo, F. Bourgeois, T. Chokshi, N. J. Durr, M. A. Hilliard, N. Chronis and A. Ben-Yakar, *Nat Methods*, 2008, 5, 531-533.

23. M. M. Crane, J. N. Stirman, C.-Y. Ou, P. T. Kurshan, J. M. Rehg, K. Shen and H. Lu, *Nat Meth*, 2012, 9, 977-980.

24. H. Lee, M. M. Crane, Y. Zhang and H. Lu, *Integr Biol*, 2013, 5, 372-380.

25. S. R. Lockery, S. E. Hulme, W. M. Roberts, K. J. Robinson, A. Laromaine, T. H. Lindsay, G. M. Whitesides and J. C. Weeks, *Lab Chip*, 2012, 12, 2211-2220.

26. G. M. Lees and D. I. Wallis, *Br J Pharmacol*, 1974, 50, 79-93.

27. S. Maruo, O. Nakamura and S. Kawata, *Optics Letters*, 1997, 22, 132-134.

28. B. H. Cumpston, S. P. Ananthavel, S. Barlow, D. L. Dyer, J. E. Ehrlich, L. L. Erskine, A. A. Heikal, S. M. Kuebler, I. Y. S. Lee, D. McCord-Maughon, J. Q. Qin, H. Rockel, M. Rumi, X. L. Wu, S. R. Marder and J. W. Perry, *Nature*, 1999, 398, 51-54.

29. A. Ostendorf and B. N. Chichkov, *Photon Spectra*, 2006, 40, 72-+.

30. B. H. Cumpston, S. P. Ananthavel, S. Barlow, D. L. Dyer, J. E. Ehrlich, L. L. Erskine, A. A. Heikal, S. M. Kuebler, I. Y. S. Lee, D. McCord-Maughon, J. Q. Qin, H. Rockel, M. Rumi, X.-L. Wu, S. R. Marder and J. W. Perry, *Nature*, 1999, 398, 51-54.

- 
31. S. Wu, J. Serbin and M. Gu, *J Photochem Photobiol A: Chem*, 2006, 181, 1-11.
32. J. Dillon, I. Andrianakis, K. Bull, S. Glautier, V. O'Connor, L. Holden-Dye and C. James, *Plos One*, 2009, 4, e8482.
- 5 33. P. E. Urwin, H. J. Atkinson, D. A. Waller and M. J. McPherson, *The Plant Journal*, 1995, 8, 121-131.
34. P. H. Mitchell, K. Bull, S. Glautier, N. A. Hopper, L. Holden-Dye and V. O'Connor, *Pharmacogenomics J*, 2007, 7, 411-417.
35. A. G. Vidal-Gadea, S. Davis, L. Becker and J. T. Pierce-Shimomura,  
10 *Worm*, 2012, 1, 5-11.
36. R. N. Rolfe and R. N. Perry, *Nematology*, 2001, 3, 31-34.
37. C. Franks, L. Holden-Dye, K. Bull, S. Luedtke and R. Walker, *Invert Neurosci*, 2006, 6, 105-122.

15